MOLEKUL
eISSN: 2503-0310

Articles

https://doi.org/10.20884/1.jm.2024.19.3.11717

Exploring The Inhibition of SARS-COV-2 PLpro: Docking and Molecular Dynamics Simulation of Flavonoid in Red Fruit Papua and Its Derivatives

Agus Dwi Ananto[1,2], Harno Dwi Pranowo[1*], Winarto Haryadi[1], Niko Prasetyo[1]

[1]Department of Chemistry, Faculty of Mathematics and Natural Sciences Universitas Gadjah Mada, Yogyakarta, Indonesia
[2]Department of Pharmacy, Faculty of Medicine and Health Science, Universitas Mataram, Mataram, Indonesia

*Corresponding author email: harnodp@ugm.ac.id

Received May 16, 2024; **Accepted** September 21, 2024; **Available online** November 20, 2024

ABSTRACT. In early 2024, Covid-19 witnessed a substantial decline in cases. Nevertheless, with lingering cases and fatalities persisting, it remains crucial to focus on research to develop patented medicines to inhibit the spread of this virus effectively. This study focuses on the Papain-like protease (PLpro) of SARS-CoV-2 because of its crucial role in the viral life cycle, where it is vital for processing precursor proteins into functional components required for viral replication and propagation. This study investigated the inhibitory potential of flavonoid compounds derived from red fruit (*Pandanus conoideus* Lam) and their derivatives against SARS-CoV-2 PLpro. Employing an in silico approach through molecular docking and MD simulation, internal validation was conducted by redocking the native ligand 100 times, resulting in an average RMSD of 0.228. The Molecular Docking stage conducted for all flavonoid compounds found in red fruit revealed that Quercetin 3′-glucoside exhibited a binding energy of -8.2440 Kcal/mol, surpassing its comparators, remdesivir and paxlovid, which recorded binding energies of -8.2590 Kcal/mol and -7.2170 Kcal/mol, respectively. Consequently, Quercetin 3′-glucoside was selected as a reference compound for identifying derivative compounds. Subsequently, a derivative compound coded DN5 (2-hydroxy-5-(3,5,7-trihydroxy-4-oxo-4H-chromen-2-yl)phenyl 2-methoxybenzoate) was obtained, demonstrating a higher binding energy than the reference compound, remdesivir, and paxlovid, with a value of -8.9300 Kcal/mol. Molecular dynamic simulations over 100 ns at 300 K further validated the stability of DN5's structure, supported by the presence of hydrogen bonds, van der Waals bonds, and several other bonds, underscoring its potential to inhibit SARS-CoV-2 PLpro and positioning it as a promising candidate for drug development.

Keywords: Docking, MD Simulation, red fruit, SARS-CoV-2 PLpro.

INTRODUCTION

In late 2019, A pivotal event that unfolded in the Chinese city of Wuhan drastically altered the course of the world: the emergence of a novel virus, later identified as SARS-CoV-2, heralded the onset of a global pandemic that reverberated across every facet of human existence (Wang, C et al. 2020; Wu F. et al., 2020; Zhu et al., 2020). Coronavirus strains have a notable history of causing epidemics, as evidenced by previous occurrences such as SARS-CoV in 2002 and MERS-CoV in 2012 (Goldsmith et al. 2004; de Groot et al. 2013; Lu et al. 2020). Since then, the world has witnessed numerous outbreaks and health crises, impacting millions worldwide.

Although SARS-CoV-2 has a lower mortality rate, it exhibits a higher transmission efficiency compared to SARS-CoV and MERS-CoV. This underscores that while the mortality rate may not be as severe as in previous pandemics, the rapid and widespread transmission of SARS-CoV-2 has led to profound social, economic, and health repercussions worldwide. With its high transmission rate, the virus swiftly disseminated from person to person, precipitating significant shifts in our lifestyles, work environments, and interpersonal interactions (Madewell et al., 2020; Patel et al., 2020). SARS-CoV-2 primarily infects the lungs, resulting in various symptoms, from asymptomatic or mild flu-like symptoms to severe cases causing lung injury (Chen et al., 2020; Huang et al., 2020).

Even though concerted efforts to mitigate the impact of the virus through measures like drug repurposing and widespread vaccination campaigns, the reality remains that numerous confirmed cases and fatalities continue to occur. According to WHO data, from January 8 to February 4, 2024, the number of new COVID-19 cases worldwide decreased by 58% compared to the previous 28-day period, with over 503,000 new cases reported. During the same period, there was a 31% reduction in the number of deaths, with over 10,000 new fatalities recorded. As of February 4, 2024, the global total stood at more than 774 million confirmed cases and over seven million deaths (WHO, 2024).

In vitro studies have demonstrated that Favipiravir and Remdesivir effectively inhibit SARS-CoV-2 infection in standard Vero E6 cells (Wang, M. et al., 2020). Several investigations have assessed the efficacy of different antiviral drugs for treating SARS-CoV-2, including hydroxychloroquine (Mahevas et al., 2020), Lopinavir-Ritonavir and Ribavirin (Hung et al., 2020), Remdesivir (Wang, Y. et al., 2020), and Tocilizumab (Xu et al., 2020). The U.S. FDA has authorized the use of Nirmatrelvir and Ritonavir (Paxlovid) to treat mild to moderate COVID-19 in adults and children (FDA, 2022).

In addition to synthetic drugs, Empirical evidence suggests that herbal plants hold promise as an alternative therapy for SARS-CoV-2 (Yang et al., 2020; Ren et al., 2020). Indonesia, renowned for its diverse flora, significantly contributes to this field. One such plant is the red fruit (*Pandanus conoideus* Lam), which possesses various medicinal properties. Native to Papua, Indonesia, the red fruit plant boasts a range of benefits, including antiparasitic, antioxidant, immunomodulatory, antitumor, and anti-HIV effects (Felle et al., 2013; Tafor et al., 2013; Tambaip et al., 2018). Previous research underscores the potential of flavonoid compounds found in red fruit as effective agents in inhibit SARS-CoV-2 (Jo et al., 2020).

Applying in silico methods for predicting the antiviral potency of herbal plant compounds offers a swift and accurate way to select diverse compounds. It presents a cost-effective and time-saving alternative to traditional drug discovery processes. Furthermore, in light of the urgent need for Covid-19 antiviral testing, adhering strictly to Biosafety Level 3 (BSL-3) standards in laboratory settings is imperative to guarantee both safety and precision in experimental outcomes (Prieto-Martínez et al., 2018).

Molecular docking and MD simulation are in silico methods for studying molecular interactions. Molecular docking enables researchers to forecast interactions between target molecules, like viral proteins and candidate compounds. In contrast, molecular dynamics simulations allow them to grasp structural changes and dynamics of compounds during interactions with their targets. Through these methods, researchers can pinpoint potential compounds capable of inhibiting viral activity with remarkable precision and efficiency, hastening the drug development process and unveiling new therapies to combat persistent viral threats (Lin *et al.,* 2020; Rachmania *et al., 2018;* Masone and Grosdidier, 2014; Childers and Daggett, 2017 and Ahmed *et al., 2013*).

Therefore, this study aims to investigate the flavonoid compounds present in red fruit and their derivatives, concentrating on their potential to inhibit SARS-CoV-2 PLpro, while also ensuring the stability of their molecular structures. The choice to focus on PLpro as an inhibitory target was influenced by its crucial role as a protease involved in the maturation of viral proteins through the cleavage of nonstructural proteins (nsp). This decision was guided by the essential function of PLpro in the viral life cycle, where it centrally participates in the processing of precursor proteins into vital components necessary for viral replication and dissemination (Amin et al. 2021; Kuo et al. 2021; Yu et al. 2022).

The inquiry begins with molecular docking, a computational method to forecast the binding affinity and interactions between these compounds and viral proteins. Following this, molecular dynamics (MD) simulations, spanning up to 100 nanoseconds, are executed to delve deeper into the dynamic behaviour and stability of the molecular complexes established during the docking phase.

EXPERIMENTAL SECTION

Material

The research was performed on a PC with an Intel Core i7-13700KF processor and 64 GB of RAM, and it utilized the Linux operating system. The primary software applications utilized were YASARA-Structure 23.8.19 (Krieger et al., 2002) and Discovery Studio Visualizer (DSV) 21.1.0.20298 (Biovia, 2020), with all software maintained at its default settings. Additionally, the research incorporated the SARS-CoV-2 PLpro crystal structure, identified by PDB ID: 7jir (Osipiuk et al., 2021).

Preparation of Ligand and Protein Target

The structural data for SARS-CoV-2 PLpro (PDB ID: 7jir) was obtained from the Protein Data Bank (Osipiuk et al., 2021). The structure was then prepared using Yasara-Structure tools, which involved removing water molecules and ions. The native ligand, TTT (5-amino-2-methyl-N-[(1R)-1-naphthalen-1-ylethyl]benzamide), was retained to benchmark the potential of herbal bioactive compounds as competitive inhibitors, while water molecules and ions were excluded. To ensure the docking procedure was accurate, 100 redocking iterations of the native ligand were carried out using additional plug-ins in Yasara-Structure. The preparation included separating the protein from its native ligand and generating the *7jir_receptor.sce* and *7jir_ligand.yob files*. Subsequently, all alterations to compound configurations undergo energy minimization using the steepest descent method before advancing to the molecular docking phase (Cavasotto & Phatak, 2009).

The flavonoid compounds present in red fruit were identified in the study by Suprijono et al. (2019), which listed eight compounds (see Table 1). These compounds were subsequently downloaded from the PubChem database (pubchem.ncbi.nlm.nih.gov). To enhance the accuracy of predicting molecular interactions and binding affinities, all flavonoid compounds underwent energy minimization.

Molecular Docking

Binding energy calculations were carried out using Yasara-Structure, which employs a force field scoring

function for docking. This process involved running a macro command (dock_run.mcr) within the Yasara-Structure platform. To facilitate the docking, Yasara-Structure automatically generated a cubic box with a 5.0 Å radius around the native ligand. The Vina docking method, incorporated into Yasara-Structure, was employed to calculate the binding energy and identify the receptor residues involved in the interaction. Following the docking process, the results were saved in PDB (.pdb) file format. The data obtained were then analyzed and visualized using Discovery Studio Visualizer application (Biovia, 2020)..

The red fruit of Papua, scientifically known as *Pandanus conoideus* Lam, has been noted for its flavonoid content, as detailed in **Table 1** (Suprijono et al., 2019). The docking analysis was performed on all the flavonoid derivatives derived from red fruit. The derivative flavonoid compound with the best docking score and hydrogen bond interactions at the active site was subsequently selected as the lead compound for designing new compounds. The newly developed compounds were then docked against the target receptor.

Molecular Dynamics (MD) simulation

MD simulations were conducted on a Linux platform using Yasara-Structure, with the macro command (*md_runmembrane.mcr*) overseeing and managing the various simulation processes. During the preparation phase, the conditions were maintained at 300 K of temperature, 7.4 of pH, and a pressure of 1 bar. A cubic simulation cell filled with water was set up, periodic boundary conditions were applied, and the membrane box was configured to be 30 Å larger than the protein, while the water box was 20 Å larger. The simulation included 0.9% NaCl ions and employed the AMBER14 force field. (Nugraha and Istyastono, 2021; Nugraha et al., 2022). With a timestep of 2.5 fs, the simulation produced data saved in .sim files over a duration of 100 ns. Following the simulation, RMSD values were computed using macro command (*md_analyze.mcr* and *BEcalculation.mcr*) to evaluate the binding free energy.

The molecular dynamics analysis demonstrated a high level of stability in the binding free energy, which was thoroughly validated through rigorous internal testing. This process included conducting 1000 redocking iterations to compare the docked poses and calculate RMSD values in relation to the ligand poses (Nugraha and Istyastono, 2021; Nugraha et al., 2022).

RESULTS AND DISCUSSION

Preparation of Ligand and Protein Target

This study retrieved the protein crystal structure with PDB ID: 7jir from *rcsb.org* (Osipiuk et al., 2021). The Yasara-structure application was employed to separate native ligands from proteins, resulting in the preservation of the native ligand as the file *7jir_ligand.yob* and the protein as the file *7jir_receptor.sce*.

The docking method was validated through 100 redocking iterations with the native ligand. The obtained result indicated an average RMSD value of 0.228 Å (**Figure 1**), confirming the validity of the docking method employed, as an RMSD value below 2 Å is generally considered reliable for ensuring the accuracy of the docking simulation (Moustakas et al., 2006).

Molecular Docking

The molecular docking phase began with the energy minimization of all flavonoid compounds. This docking process was also conducted for comparative compounds, namely remdesivir and paxlovid. Quercetin 3'-glucoside has the lowest binding energy value (-8.2440 Kcal/mol) among all the flavonoid compounds identified. **Figure 2** illustrates the two-dimensional structure of the compound quercetin 3'-glucoside. Based on the docking results, quercetin 3'-glucoside was selected as a lead compound for the development of new drug candidates.

In this study, a total of 24 new compounds were designed and successfully docked. Supplementary **Table 1** displays the 2D structures of all designed compounds. Based on the conducted docking results, the design compound numbered 5 with code DN5 (2-hydroxy-5-(3,5,7-trihydroxy-4-oxo-4H-chromen-2-yl)phenyl 2-methoxybenzoate) obtained the best binding energy value of -8.9300 Kcal/mol. Details regarding the docking scores and contacting receptor residues can be found in **Table 1**. **Figure 3**(**a**) illustrates one of the molecular docking processes. **Figures 3**(**b**), **3**(**c**), and **3**(**d**) sequentially show 2D interaction diagrams between the native ligand and the receptor, remdesivir and the receptor, and DN5 and the receptor, respectively.

In **Figure 3**(**b**), hydrogen bonds are seen between the ligand and the amino acid residues ASP164 and GLN269. In **Figure 3**(**c**), hydrogen bonds are seen between the ligand and the amino acid residues LEU162, ARG166, and TYR268. Meanwhile, in **Figure 3**(**d**), hydrogen bonds are found between the ligand and the amino acid residues GLU167 and GLN269. Studies by Gao et al. (2020) and Calleja et al. (2022) have shown that hydrogen bonds with amino acid residues, such as GLN269 near the active site, can stabilize the inhibitor-PLpro complex and enhance the inhibition of SARS-CoV-2 PLpro. Therefore, the proposed compound DN5 shows the most significant potential as a new candidate for PLpro inhibition, not only because it exhibits the lowest binding energy but also because it forms hydrogen bonds with amino acid residues that play a crucial role in the inhibition of SARS-CoV-2 PLpro. However, further molecular dynamics simulations are necessary to evaluate the stability of the proposed DN5 compound within the body.

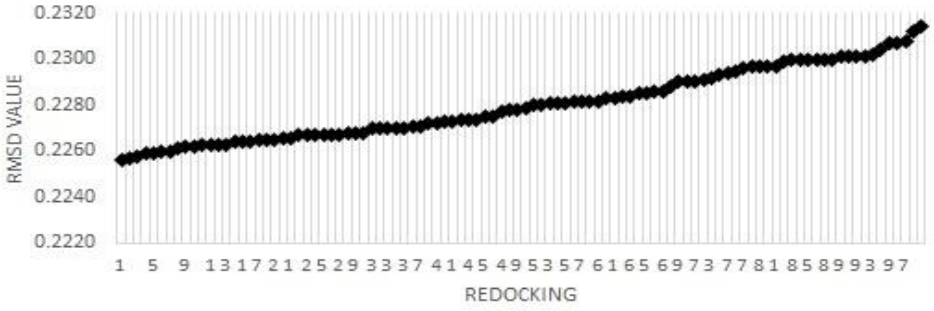

Figure 1. RMSD value for validation by redocking 100 time

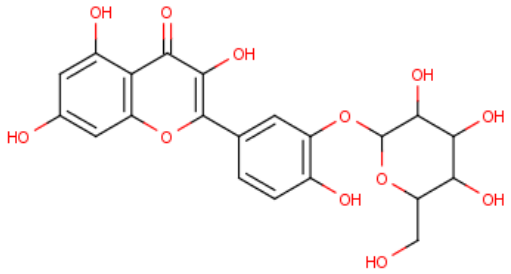

Figure 2. Two-dimensional structure of quercetin 3'-glucoside as the lead compound

Table 1. Binding energy value and Interacting receptor residue from docking molecular result of flavonoid in red fruit Papua and one of the best docking results for its derivative

No	Ligand	Binding Energy (Kcal/mol)	Interacting receptor residues
1	4',6,6',8-tetrahydroxy-3-methoxy-flavon	-6.3500	ASP164 VAL165 ARG166 MET208 ALA246 PRO247 PRO248 TYR264 GLY266 ASN267 TYR268 **GLN269** TYR273 THR301
2	3,4',5-trihydroxy-7,3'-dimethoxy flavon	-6.4100	LYS157 LEU162 GLY163 ASP164 ARG166 GLU 167 MET208 ALA246 PRO247 PRO248 TYR264 TYR268 **GLN269** TYR273
3	Taxifolin 3-O-α-arabinopyranose	-7.2380	LEU162 GLY163 ASP164 ARG166 GLU167 MET208 SER245 ALA246 PRO247 PRO248 TYR264 ASN267 TYR268 **GLN269** TYR273 THR301
4	Quercetin 3-O-glucose	-7.2990	ASP164 ARG166 MET208 SER245 ALA246 PRO247 PRO248 TYR264 GLY266 ASN267 TYR268 TYR273 THR301 ASP302
5	Quercetin 3-methyl-ether	-7.1110	LYS157 LEU162 GLY163 ASP164 ARG166 GLU167 MET208 ALA246 PRO247 PRO248 TYR264 TYR268 **GLN269** TYR273 THR301
6	Quercetin	-6.8470	ASP164 VAL165 ARG166 MET208 PRO247 PRO248 TYR264 GLY266 ASN267 TYR268 TYR273 THR301 ASP302
7	Taxifolin	-6.6140	ASP164 ARG166 GLU167 MET208 SER245 ALA246 PRO247 PRO248 TYR264 GLY266 ASN267 TYR268 THR301
8	Quercetin 3'-glucoside	-8.2440	LYS157 LEU162 GLY163 ASP164 ARG166 GLU167 MET208 ALA246 PRO247 PRO248 TYR264 GLY266 ASN267 TYR268 **GLN269** TYR273 THR301
9	Ligand native	-7.5170	ASP164 ARG166 MET208 PRO247 PRO248 GLN250 TYR264 THR265 GLY266 ASN267 TYR268 **GLN269** TYR273 PRO299 THR301
10	Remdesivir	-7.4420	LYS157 LEU162 GLY163 ASP164 PRO247 PRO248 TYR264 THR265 GLY266 ASN267 TYR268 **GLN269** GLY271 TYR273 PRO299 THR 301
11	Paxlovid	-7.2170	ASP164 ARG166 GLU167 MET208 ALA246 PRO247 PRO248 TYR264 GLY266 ASN267 TYR268 **GLN269** TYR273 PRO299 THR301
12	DN5	-8.9300	LYS157 LEU162 GLY163 ASP164 ARG166 GLU167 MET208 SER245 ALA246 PRO247 PRO248 TYR264 TYR268 **GLN269** CYS270 GLY271 TYR273 THR301 ASP302

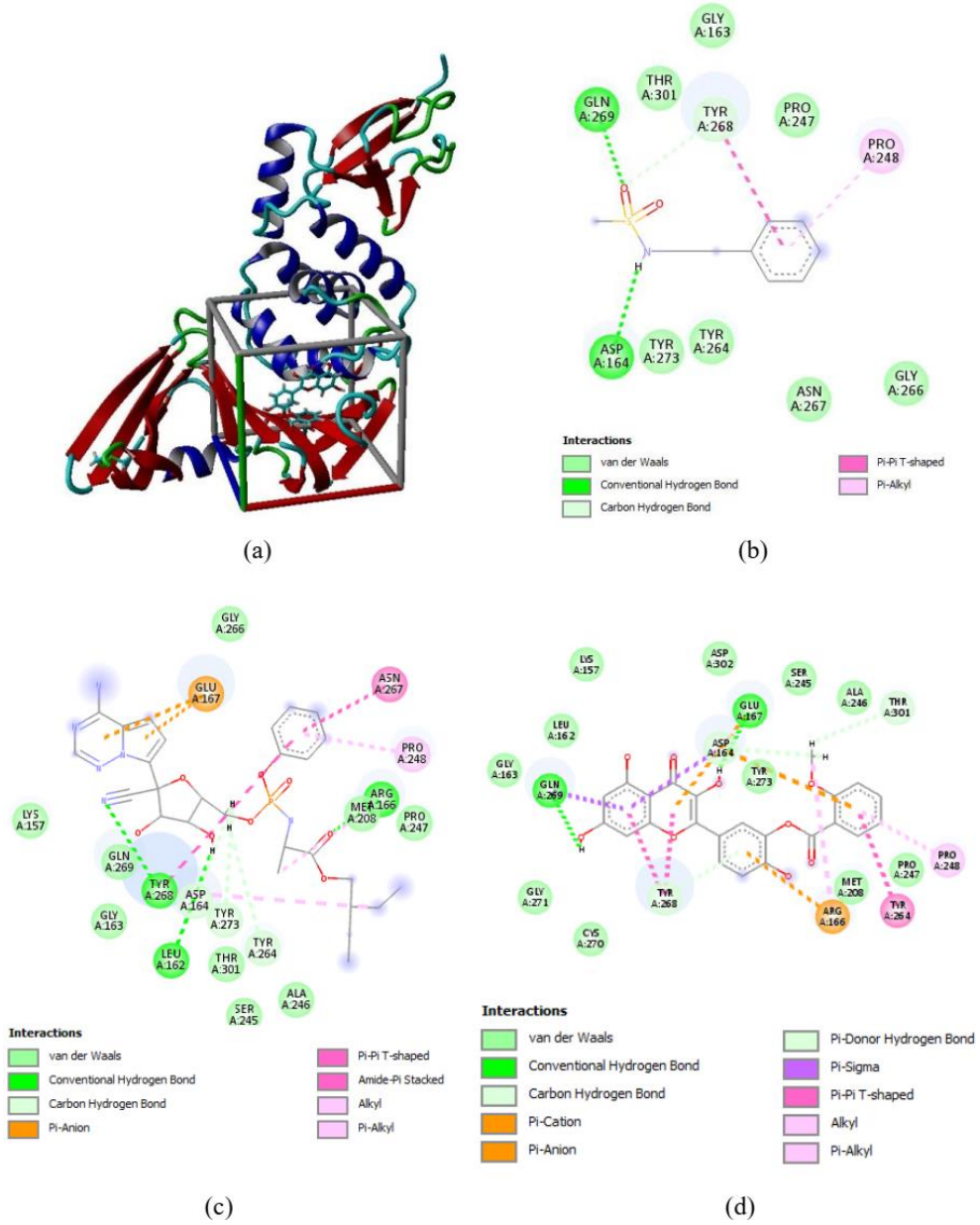

Figure 3. (**a**) An example of the docking process; (**b**) 2D visualisation of the interactions between the native ligand and amino acid residues; (**c**) 2D visualisation of the interactions between remdesivir and amino acid residues; (**d**) 2D visualisation of the interactions between the proposed compound DN5 and amino acid residues.

MD Simulation

Understanding molecular interactions is essential for assessing the stability of ligand-protein complexes. While docking provides an initial understanding of these interactions, it often omits certain factors, such as including water molecules. However, molecular dynamics (MD) simulation addresses this gap by incorporating water and other environmental factors, making it a potent tool for unravelling such intricacies. By subjecting the complex to virtual dynamic environments, including water, MD simulations provide valuable insights into its behaviour over time, offering a more comprehensive understanding of its stability. In this context, the MD simulation not only elucidates the complex's stability but also enables the calculation of critical parameters essential for characterising its dynamics. Following the simulation, analysis techniques such as Root Mean Square Deviation (RMSD) and free-binding energy calculations are employed. These analyses, derived from the MD simulation data, offer quantitative measures of the complex's structural deviations and thermodynamic stability. This integrated approach gives this study a comprehensive understanding of the ligand-protein interaction, paving the way for rational drug design and biochemical analyses. **Figure 4** visually depicts the ligand-protein complex, providing a clear and comprehensive visualisation of their molecular interaction.

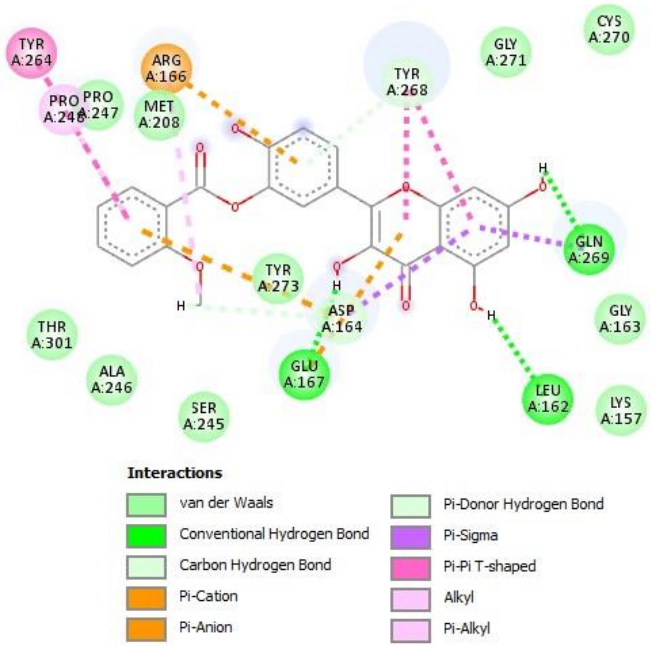

Figure 4. 2D visualisation of the interactions between the best-proposed ligand from docking results using molecular dynamics simulation

The MD process in this study employs a temperature of 300 K and is conducted for 100 ns. The researchers opted to perform molecular dynamic simulations at 300 K as it's a prevalent choice in MD simulations for mimicking room temperature, facilitating comparisons with numerous other investigations. Considering the significance of this temperature on these findings is crucial, as it could influence both the conformational variety explored by the protein and the system's stability. While enzymes are generally active at body temperature (~310 K), the use of 300 K is often justified due to its similar conformational sampling compared to 310 K (Kubitzki and de Groot, 2007; Jung et al., 2018).

Klepeis et al. (2009) emphasise that molecular dynamics simulations conducted over extended timescales are essential for comprehensively exploring protein dynamics. Such extended simulations allow for observing conformational changes that might be missed in shorter simulations. This study uses 100 ns simulation time for several reasons. Firstly, a more extended simulation period allows for a more in-depth exploration of the dynamics of complex molecules. Secondly, various molecular conformational changes can be observed more effectively within this timeframe, providing a more comprehensive understanding of the system's behaviour. Lastly, a longer simulation time also increases the chances of detecting rare events or critical conformational transitions crucial for understanding molecular function.

Visualising the ligand-protein complex presented in **Figure 4** illustrates interactions characterised by strong bonding with residues LEU162, GLU167, and GLN269 via conventional hydrogen bonds. Van der Waals interactions, along with other bonding forces, play an indirect role in inhibiting SARS-CoV-2 PLpro. Both hydrogen bonds and van der Waals interactions significantly impact the binding process. Hydrogen bonding helps stabilize the ligand within protein-ligand interactions, while hydrophobic and van der Waals forces are crucial for stabilizing nonpolar ligands. Examining the ligand structures and their docked conformations is essential for understanding these interactions and determining the binding energy of the compounds (Meng et al., 2011). Although Van der Waals interactions are often considered the weakest form of intermolecular attraction, they can become substantial when multiple forces are involved, despite their individual weakness (Barratt et al., 2005).

In **Figure 5**, it can be observed that stability begins to form after 18 ns. This indicates that the RMSD values stabilise beyond this point. This behaviour suggests that the protein-ligand complex gradually adjusts to its optimal conformation over time, reflecting the inherent dynamics and stability of the system as revealed by the MD simulation. The interpretation of structural changes, especially the differences between two structures, is most effectively done by analysing the graph generated from Root Mean Square Deviation (RMSD) calculations derived from Molecular Dynamics (MD) simulation trajectories. This computation elucidates the spatial disparities among the protein's backbone atoms throughout the simulation duration relative to the initial structure at simulation onset. Smaller disparities signify more significant spatial similarity between the compared structures, while larger RMSD values denote more considerable divergence. Consequently, a higher RMSD value indicates the protein system's instability.

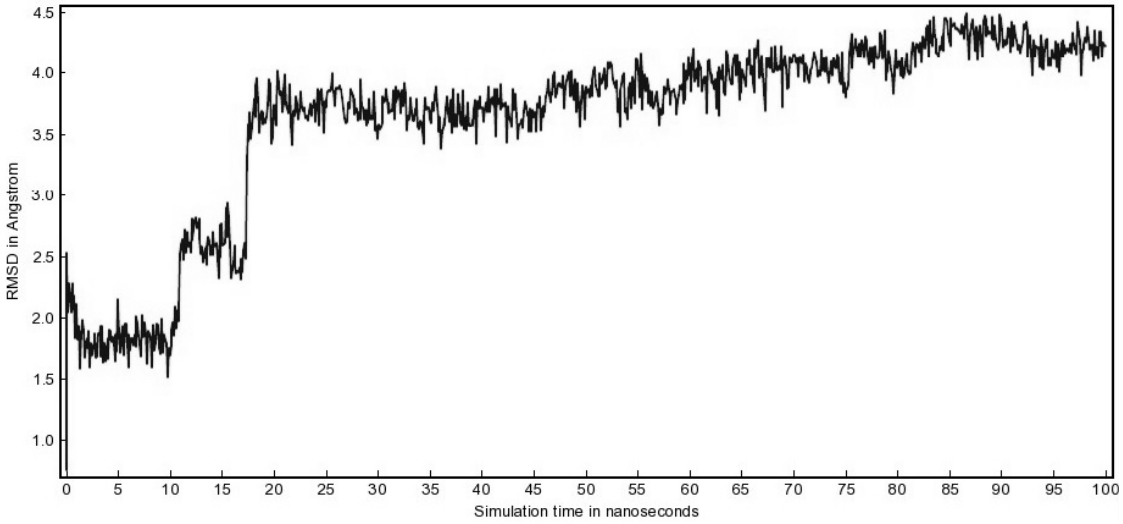

Figure 5. Ligand conformation RMSD after superposing on the ligand

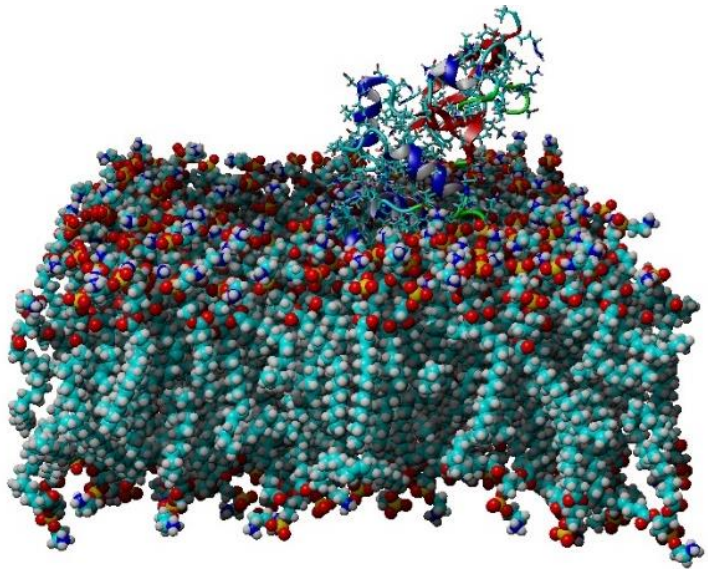

Figure 6. The system exhibiting the greatest degree of stability

Moreover, delta RMSD values were computed at 5 ns intervals, revealing that most of these values are below 1.0. Hence, molecular dynamics simulations are deemed acceptable when yielding RMSD values below 2.0 (Zhang and Aires-de-Sousa, 2007). Consequently, this metric is a gauge for assessing the structure's stability throughout the simulation. Following the 501 steps, the energy minimisation experiment was successfully concluded. Furthermore, the system, showcasing a free binding energy value of -10.0950 Kcal/mol, underscored its exceptional stability in the binding free energy calculation (**Figure 6**). Subsequently, this system was chosen as the focal point for further analysis and validation. Internal validation aimed at corroborating the efficacy of the MD simulation results entailed redocking the ligand-receptor interactions 1000 times with 25 iterations. The validation process yielded RMSD values below 2 Å (the average RMSD value is 0.779785 Å), affirming the accuracy of the results (supplementary **Table 2**).

CONCLUSIONS

This study explores the efficacy of flavonoid compounds from *Pandanus conoideus* Lam in inhibiting SARS-CoV-2 PLpro. By employing an in silico approach that includes molecular docking and molecular dynamics (MD) simulations, the research performed internal validation through 100 redocking iterations of the native ligand, achieving an average RMSD of 0.228. Molecular docking identified quercetin 3'-glucoside as having the lowest binding energy of -8.2440 Kcal/mol. Building on this, the design of new derivative compounds led to the identification of DN5 (2-hydroxy-5-(3,5,7-trihydroxy-4-oxo-4H-chromen-2-yl)phenyl 2-methoxybenzoate), which exhibited an even lower binding energy of -8.9300 Kcal/mol compared to remdesivir and paxlovid. MD simulations over 100 ns at 300 K further validated the structural stability of DN5, highlighting its interactions through hydrogen bonds, van der Waals bonds, and other interactions. Additionally, the

presence of hydrogen bonds, specifically with GLN269, supports stability in inhibiting PLpro. These findings suggest that DN5 holds significant promise as a potential inhibitor of SARS-CoV-2 PLpro and as a candidate for further drug development.

REFERENCES

Ahmed, M., Sadek, M.M., Abouzid, K.A., and Wang, F. (2013). In silico design: Extended molecular dynamic simulations of a new series of dually acting inhibitors against EGFR and HER2, *Journal of Molecular Graphics and Modelling, 44*, 220–231.

Amin SA, Banerjee S, Ghosh K, Gayen S, Jha T. (2021). Protease targeted COVID-19 drug discovery and its challenges: Insight into viral main protease (Mpro) and papain-like protease (PLpro) inhibitors. *Bioorganic & Medicinal Chemistry, 29*(August 2020):115860. doi:10.1016/j.bmc. 2020.115860.

Barratt, E., Bingham, R.J., Warner, D.J., Laughton, C.A., Phillips, S.E., Homans, S.W. (2005). Van der Waals interactions dominate ligand protein association in a protein binding site occluded from solvent water. *Journal of the American Chemical Society, 127*, 11827–11834.

Calleja, D. J., Lessene, G., & Komander, D. (2022). Inhibitors of SARS-CoV-2 PLpro. *Frontiers in Chemistry, 10*, 876212.

Cavasotto, C. N., & Phatak, S. S. (2009). "Computational methods for drug discovery." *Methods in Molecular Biology*, *478*, 161-181

Chen, N., Zhou, M., Dong, X., Qu, J., Gong, F., Han, Y., et al. (2020). Epidemiological and Clinical Characteristics of 99 Cases of 2019 Novel Coronavirus Pneumonia in Wuhan, China: a Descriptive Study. *The Lancet, 395*(10223), 507–513. doi:10.1016/s0140-6736(20) 30211-7.

Childers, M.C. and Daggett, V. (2017). Insights from molecular dynamics simulations for computational protein design, Molecular Systems Design & Engineering, *2*, 9–33.

de Groot RJ, Baker SC, Baric RS, Brown CS, Drosten C, Enjuanes L, Fouchier RAM, Galiano M, Gorbalenya AE, Memish ZA, Perlman S, Poon LLM, Snijder EJ, Stephens GM, Woo PCY, Zaki AM, Zambon M, & Ziebuhr J. (2013). Middle East Respiratory Syndrome Coronavirus (MERS-CoV): Announcement of the Coronavirus study group. *Journal of Virology, 87*(14):7790–7792. doi:10.1128/jvi.01244-13.

Fda.gov [Internet] U.S. (2024). Food & Drugs Administration: Fact sheet for healthcare providers: Emergency authorization for Paxlovid, [cited 2022 Feb 23]. Available from https://www.fda.gov/

Felle Z R, Wijayanti M A, & Supargiyono (2013). The Effect of Pandanus conoideus Lamk Extract to the Serum Level of TNF-α, IL-10 and Parasitemia of Plasmodium berghei Infected in Mice. *Tropical Medicine Journal, 3*(1), 39-47.

Gao, X., Qin, B., Chen, P., Zhu, K., Hou, P., Wojdyla, J. A., Wang, M., & Cui, S. (2020). Crystal structure of SARS-CoV-2 papain-like protease. *Acta Pharmaceutica Sinica B*, *11*(1), 237-245

Goldsmith CS, Tatti KM, Ksiazek TG, Rollin PE, Comer JA, Lee WW, Rota PA, Bankamp B, Bellini WJ, Zaki SR. (2004). Ultrastructural characterization of SARS Coronavirus. *Emerging Infectious Diseases, 10*(2):320–326. doi:10.3201/eid 1002.030913.

Huang, C., Wang, Y., Li, X., Ren, L., Zhao, J., Hu, Y., et al. (2020). Clinical features of patients infected with 2019 novel coronavirus in Wuhan, China. *The Lancet, 395* (10223), 497–506. doi:10.1016/s0140-6736(20)30183-5.

Hung, I.F.-N., Lung, K.-C., Tso, E.Y.-K., Liu, R., Chung, T.W.-H., Chu, M.-Y., Ng, Y.-Y., Lo, J., Chan, J., Tam, A.R., Shum, H.-P., Chan, V., Wu, A.K.-L., Sin, K.-M., Leung, W.-S., Law, W.-L., Lung, D.C., Sin, S., Yeung, P., et al. (2020). Triple combination of interferon beta-1b, lopinavir–ritonavir, and ribavirin in the treatment of patients admitted to hospital with COVID-19: an open-label, randomised, phase 2 trial, *The Lancet, 395*, 1695–704.

Jo, S., Kim, S., Kim, D. Y., Kim, M. S., & Shin, D. H. (2020). Flavonoids with inhibitory activity against SARS-CoV-2 3CLpro. *Journal of Enzyme Inhibition and Medicinal Chemistry*, *35*(1), 1539–1544. https://doi.org/10.1080/ 14756366.2020.1801672.

John L Klepeis, Kresten Lindorff-Larsen, Ron O Dror, David E Shaw, (2009). Long-timescale molecular dynamics simulations of protein structure and function, *Current Opinion in Structural Biology, 19*(2), 120-127, ISSN 0959-440X, https://doi.org/10.1016/j.sbi.2009.03. 004.

Jung, J., Kobayashi C., and Sugita Y. (2018). Optimal Temperature evaluation in molecular dynamics simulations with a large time step. *Journal of Chemical Theory and Computation, 15*(1), 84–94

Kubitzki M. B., and de Groot B. L. (2007). Molecular Dynamics Simulations Using Temperature-Enhanced Essential Dynamics Replica Exchange, *Biophysical Journal, 92*(12), 4262–4270.

Kuo CJ, Chao TL, Kao HC, Tsai YM, Liu YK, Wang LH, Hsieh MC, Chang SY, Liang PH. (2021). Kinetic characterization and inhibitor screening for the proteases leading to identification of drugs against SARS-CoV- 2. *Antimicrobial Agents and Chemotherapy, 65*(4): 02577–20.doi:10. 1128/AAC.02577-20.

Lin, Xiaoqian, Li, X., and Lin, Xubo (2020). A Review on Applications of Computational Methods in Drug Screening and Design. *Molecules, 25*, 1375.

Lu R, Zhao X, Li J, Niu P, Yang B, Wu H, Wang W, Song H, Huang B, Zhu N, Bi Y, Ma X, Zhan F, Wang L, Hu T, Zhou H, Hu Z, Zhou W, Zhao L, Chen J, Meng Y, Wang J, Lin Y, Yuan J, Xie Z, Ma J, Liu WJ, Wang D, Xu W, Holmes EC, Gao GF, Wu G, Chen W, Shi W, Tan W. (2020). Genomic characterisation and epidemiology of 2019 novel coronavirus: Implications for virus origins and receptor binding. *The Lancet 395*(10224): 565–574. doi:10.1016/S0140-6736(20)30251-8.

Madewell, Z. J., Yang, Y., Longini, I. M., Jr., Halloran, M. E., and Dean, N. E. (2020). Household Transmission of SARS-CoV-2. *JAMA Network Open, 3*(12), e2031756. doi:10.1001/ jamanetworkopen.2020.31756.

Mahevas, M., Tran, V.-T., Roumier, M., Chabrol, A., Paule, R., Guillaud, C., Fois, E., Lepeule, R., Szwebel, T.-A., Lescure, F.-X., Schlemmer, F., Matignon, M., Khellaf, M., Crickx, E., Terrier, B., Morbieu, C., Legendre, P., Dang, J., Schoindre, Y., et al. (2020) Clinical efficacy of hydroxychloroquine in patients with covid-19 pneumonia who require oxygen: observational comparative study using routine care data. *BMJ: British Medical Journal, 1844.* doi: https://doi.org/10.1101/2020.04.10.20060699

Masone, D. and Grosdidier, S., 2014, Collective variable driven molecular dynamics to improve protein–protein docking scoring. *Computational Biology and Chemistry, 49,* 1–6.

Meng, X.Y., Zhang, H.X., Mezei, M., Cui, M., 2011. Molecular docking: a powerful approach for structure-based drug discovery. *Current Computer-Aided Drug Design, 7*, 146–157

Moustakas DT, Lang PT, Pegg S, Pettersen E, Kuntz ID, Brooijmans N, Rizzo RC. (2006). Development and validation of a modular, extensible docking program: DOCK 5. *Journal of Computer-Aided Molecular Design, 20*(10-11):601-19. doi: 10.1007/s10822-006-9060-4. Epub 2006 Dec 6. PMID: 17149653.

Nugraha G, Istyastono EP. (2021). Virtual target construction for structure-based screening in the discovery of histamine H2 receptor ligands. *International Journal of Applied Pharmaceutics, 13*, 239-41.

Nugraha, G., Pranowo, H. D., Mudasir, M., & Istyastono, E. P., (2022). Virtual Target Construction for Discovery of Human Histamine H4 Receptor Ligands Employing a Structure-Based Virtual Screening Approach. *International Journal of Applied Pharmaceutics, 2022; 14*(4), 213–18.

Osipiuk, J., Azizi, SA., Dvorkin, S. et al. (2021). Structure of papain-like protease from SARS-CoV-2 and its complexes with non-covalent inhibitors. *Nature Communications, 12*,743 (2021).

Patel, K. P., Vunnam, S. R., Patel, P. A., Krill, K. L., Korbitz, P. M., Gallagher, J. P., et al. (2020). Transmission of SARS-CoV-2: an Update of Current Literature. *European Journal of Clinical Microbiology & Infectious Diseases, 39*(11), 2005–2011. doi:10.1007/ s10096-020-03961-1.

Prieto-Martínez, F.D., Arciniega, M., and Medina-Franco, J.L. (2018). Acoplamiento molecular: Avances Recientes y Retos. *TIP Revista Especializada en Ciencias Químico-Biológicas*, *21*, 65-87.

Rachmania, R.A., Hariyanti, H., Zikriah, R., and Sultan, A. (2018). Studi in silico senyawa alkaloid herba bakung putih (*Crinum asiaticum* L.) pada penghambatan enzim siklooksigenase (COX) (In silico study of the alkaloid compounds of the white lily (*Crinum asiaticum* L.) herb on the inhibition of the cyclooxygenase (COX) enzyme). *Jurnal Kimia VALENSI*, *4*, 124–136.

Ren, J., Zhang, A.-H., and Wang, X.-J. (2020). Traditional Chinese medicine for COVID-19 treatment. *Pharmacological Research, 155*, 104743.

Suprijono MM, Widjanarko SB, Sujuti H, Kurnia D (2019). Computational study of antioxidant activity and bioavailability of papua red fruit (Pandanus conoideus Lam.) flavonoids through docking toward human serum albumin. *AIP Conference Proceedings, 2108*(020020). https://doi.org/10.1063/1. 5109995

Tafor D, Djunaidi A, Wasityastuti W, and Solikhah E N. (2013). Tumor Necrosis Factor-Alpha (TNF-Alpha) And Intercellular Adhesion Molecule-1 (ICAM-1) Expression of Plasmodium Berghei Infected Swiss Mice Treated with Red Fruit (Pandanus Conoideus Lam) Ethanol Extract, *Tropical Medicine Journal, 3*, 155-65.

Tambaip, T., Br Karo, M., Hatta, M., Dwiyanti, R., Natzir, R., Nasrum Mas, M., Asadul Isl, A., and Djawad, K. (2018). Immunomodulatory Effect of Orally Red Fruit (Pandanus conoideus) Extract on the Expression of CC Chemokine Receptor 5 mRNA in HIV Patients with Antiretroviral Therapy, *Research Journal of Immunology, 11*, 15–21.

Wang C, Horby PW, Hayden FG, Gao GF. 2020. A novel coronavirus outbreak of global health concern. *The Lancet, 395*(10223):470–473. doi:10.1016/S0140-6736(20)30185-9);

Wu, F., Zhao, S., Yu, B., Chen, Y.-M., Wang, W., Song, Z.-G. (2020a). A New Coronavirus

Associated with Human Respiratory Disease in China. *Nature, 579*(7798), 265–269. doi:10.1038/s41586-020-2008-3.

Wang, M., Cao, R., Zhang, L., Yang, X., Liu, J., Xu, M., Shi, Z., Hu, Z., Zhong, W., and Xiao, G., (2020). Remdesivir and chloroquine effectively inhibit the recently emerged novel coronavirus (2019-nCoV) in vitro. *Cell Research, 30*, 269–71.

Wang, Y., Zhang, D., Du, G., Du, R., Zhao, J., Jin, Y., Fu, S., Gao, L., Cheng, Z., Lu, Q., Hu, Y., Luo, G., Wang, K., Lu, Y., Li, H., Wang, S., Ruan, S., Yang, C., Mei, C. (2020). Remdesivir in adults with severe COVID-19: a randomised, double-blind, placebo-controlled, multicentre trial. *The Lancet, 395*, 1569–578.

WHO.int [Internet] covid-19-epidemiological [cited 2024 Feb 16]. Available from https://www.who.int/publications.

Xu, X., Han, M., Li, T., Sun, W., Wang, D., Fu, B., Zhou, Y., Zheng, X., Yang, Y., Li, X., Zhang, X., Pan, A., and Wei, H. (2020). Effective treatment of severe COVID-19 patients with tocilizumab, *Proceedings of the National Academy of Sciences, 117*, 10970–975.

Yang, Y., Islam, M.S., Wang, J., Li, Y., and Chen, X. (2020). Traditional Chinese Medicine in the Treatment of Patients Infected with 2019-New Coronavirus (SARS-CoV-2): A Review and Perspective. *International Journal of Biological Sciences, 16*, 1708–1717.

Yu W, Zhao Y, Ye H, Wu N, Liao Y, Chen N, Li Z, Wan N, Hao H, Yan H, Xiao Y, Lai M. (2022). Structure-based design of a dual-targeted covalent inhibitor against papain-like and main proteases of SARS-CoV-2. *Journal of Medicinal Chemistry, 65*(24), 16252–16267. doi:10. 1021/ acs.jmedchem.2c00954.

Zhang QY, Aires-de-Sousa J. (2007). Random forest prediction of mutagenicity from empirical physicochemical descriptors. *Journal of Chemical Information and Modeling, 47*(1):1-8. doi: 10.1021/ ci050520j. PMID: 17238242.

Zhu, N., Zhang, D., Wang, W., Li, X., Yang, B., Song, J., et al. (2020). A Novel Coronavirus from Patients with Pneumonia in China, 2019. *The New England Journal of Medicine, 382*(8), 727–733. doi:10.1056/ nejmoa2001017.